A time dependent model for unidirectional fibre-reinforced composites with viscoelastic matrices

Boumediene Nedjar

A time dependent model for unidirectional fibre-reinforced composites with viscoelastic matrices

B. Nedjar[a]

[a]*Université Paris-Est, Laboratoire Navier (ENPC/IFSTTAR/CNRS)*
Ecole des Ponts ParisTech
6 et 8 avenue Blaise Pascal, 77455 Marne-la-Vallée, France

Abstract

In this work, a fully three-dimensional constitutive model suitable for the macroscopic description of unidirectional fibre-reinforced composites where the matrix exhibits a time-dependent viscoelastic behaviour is developed. Specifically, we consider a coordinate-free formulation where the stress and strain fields can be decomposed into fibre-directional and volumetric parts on the one hand, and into extra contributions on the other hand. This offers an ideal framework where one can separate the fibres' contribution, considered here as time-independent and linearly elastic, and the matrix contribution that experiences creep only in shear. Among the many possibilities, we choose in this work a generalized Kelvin-Voigt rheological model to formulate the viscoelastic behaviour of the matrix. Long-term as well as short-term relaxation processes can be integrated in the model by means of as many as necessary viscoelastic processes. The numerical discretization is described for an easy intergration within a finite element procedure. Finally, numerical examples illustrate the possibilities of the present model.

Keywords: Fibre reinforced composites, Transversely isotropic, Creep, Viscoelastic matrix, Finite element method.

1. Introduction

Nowadays, a wide variety of industrial applications employ fibre-reinforced materials. Typically, these materials consist of a fabric structure where the fibres are continuously arranged in a matrix material. They exhibit then strong directional properties, so that macroscopically they have to be regarded as anisotropic materials. The applications we have in mind are fibre-reinforced composites with polymer matrices and metal matrices, but the theory is not limited to any particular type of material. In this work, we focus our attention to the particular case of unidirectional fibre-reinforced composites. When a material is reinforced with one family of fibres, it has a single preferred direction and so is transversely isotropic with respect to this direction.

In many cases, matrix creep can occur. As the role of the matrices is essentially to deform and support stresses primarly in shear, it becomes then important to consider this particularity within a phenomenological modelling framework. In this paper, the anisotropic behaviour is captured by a constitutive equation formulated in terms of the so-called integrity basis as proposed by Spencer (1984), and widely employed in the finite strain range, see for example (Bonet and Burton, 1998; Holzapfel, 2000; Reese et al., 2001; Weiss et al., 1996) for purely elastic materials, and (Holzapfel, 2000; Kaliske, 2000; Klinkel et al., 2005; Nedjar, 2007; Reese, 2003; Sansour et al., 2006) for anelastic materials to mention few. The stress-strain constitutive relation can be decomposed into a volumetric and fibre-directional parts on the one hand, and into an extra-stress-strain part where the shear contribution is

2

extracted, on the other hand. The key idea in this work is that the constitutive equation is chosen to be viscoelastic only on the extra-stress part of the total stress field, while the remainder part of the stress remains fully elastic. Among the many possibilities, the present viscoelastic formulation is motivated by the classical generalized Kelvin-Voigt rheological model. In the developments below, we choose to characterize such a behaviour by means of an internal variable model even if a description with external variables is also possible. The time integration of the local evolution equations is addressed. Within the finite element framework this latter is performed at the intergration points level. Two finite difference schemes are presented and fully detailed.

The continuum approach presented in this work is developed within the infinitesimal theory under the small perturbations assumption. It excludes any consideration of the micro-mechanics of the composites. This is in fact an important problem which involves interactions between individual fibres and the matrix, see for example (Beyerlein et al., 1998; Ohno et al., 2002) among many others. There are many important problems on micro-scale, but these will not be considered here.

The paper is organized as follows. In Section 2, the alternative formulation of transversely isotropic constitutive relation as proposed by Spencer (1984) is outlined. The composite is viewed as locally transversely isotropic with respect to the known local fibres' direction which is not necessarily the same at each point. Moreover, this formulation motivates the decomposition of the stress-strain relation into a fibre-directional, a volumetric, and an extra-stress-strain parts. This latter is extended to incorporate viscoelas-

ticity in Section 3 through a generalized Kelvin-Voigt rheological model via an internal variable formulation. In Section 4, two alternative time integration schemes are detailed to approximate the local evolution equations of viscoelasticity within a finite element framework. Then a set of representative numerical examples is given in Section 5. In particular, we study the sensitivity of the model with regards to slight off-axis loadings. Finally, conclusions and perspectives are drawn in Section 6. Noteworthy remarks and comments are given throughout this paper.

2. Motivation. Linear elasticity framework

When an isotropic material is reinforced with a single family of fibres, the resulting composite material becomes transversely isotropic with respect to the single preferred direction of the fibres. In what follows, we denote by $\vec{V}_F$ the *unit* vector that characterizes this fibre direction. This vector is regarded as a continuous function of the position $\boldsymbol{x}$. Moreover, we introduce the structural tensor defined by the dyadic product as $\boldsymbol{M}_F = \vec{V}_F \otimes \vec{V}_F$, which is a second-order tensor field of the micro-structure. The symbol $\otimes$ denotes the tensor product, *i.e.* with components $M_{F_{ij}} = V_{F_i} V_{F_j}$. For later use, notice the useful algebraic property that this structural tensor is idempotent, *i.e.* $\boldsymbol{M}_F^n = \boldsymbol{M}_F$ for any value of the positive integer n.

In the general case of fibre-reinforced materials, Spencer (1984) developed a constitutive strain energy function in terms of invariants. For the particular case with one family of fibres, he extended the basis of three characteristic quantities of isotropy to five irreducible invariants of transverse isotropy. The standard constitutive equation in linear elasticity relating the stress

4

tensor $\boldsymbol{\sigma}$ and the infinitesimal strain tensor $\boldsymbol{\varepsilon}$ is then found to be equivalently given by

$$
\begin{aligned}
\boldsymbol{\sigma} \;=\;& \lambda \operatorname{tr}[\boldsymbol{\varepsilon}]\,\mathbf{1} + 2\mu_T\,\boldsymbol{\varepsilon} + \alpha\,([\boldsymbol{\varepsilon}:\boldsymbol{M}_F]\,\mathbf{1} + \operatorname{tr}[\boldsymbol{\varepsilon}]\,\boldsymbol{M}_F) \\
+\;& \beta\,[\boldsymbol{\varepsilon}:\boldsymbol{M}_F]\,\boldsymbol{M}_F + 2(\mu_L - \mu_T)\,\{\boldsymbol{M}_F\,\boldsymbol{\varepsilon} + \boldsymbol{\varepsilon}\,\boldsymbol{M}_F\}
\end{aligned}
\tag{1}
$$

where the five independent material parameters λ, μ_T, μ_L, α and β are Lamé-like elastic constants, see also (Kaliske, 2000) for details. The constants μ_L and μ_T are the shear moduli on planes parallel to- and normal to- the fibres, respectively. The other constants λ, α and β can be easily related to the standard Young's moduli and Poisson's ratios as will be explained later on in Section 5. Here and in all what follows, $\mathbf{1}$ denotes the second order unit tensor with components δ_{ij} (δ_{ij} being the Kronecker delta with $\delta_{ij} = 1$ if $i = j$ and $\delta_{ij} = 0$ if $i \neq j$), $\operatorname{tr}[.]$ designates the trace operator, and the double dot symbol : denotes the double tensor contraction, $i.e.$ $\boldsymbol{A} : \boldsymbol{B} = \operatorname{tr}[\boldsymbol{A}\boldsymbol{B}^T] \equiv A_{ij}B_{ij}$ where summation on repeated indices is assumed here. In particular, one has $\operatorname{tr}[(.)] = (.) : \mathbf{1}$. And for later use, the tensor product of two second order tensors $\boldsymbol{A}$ and $\boldsymbol{B}$ is the fourth-order tensor with components $(\boldsymbol{A} \otimes \boldsymbol{B})_{ijkl} = A_{ij}B_{kl}$.

By analogy with Spencer's plasticity theory for materials reinforced with one family of fibres (Spencer, 1984), the stress tensor can be decomposed as

$$
\boldsymbol{\sigma} = \boldsymbol{s} + p\,\mathbf{1} + T\,\boldsymbol{M}_F
\tag{2}
$$

where the scalar stress quantities p and T are determined by imposing the conditions

$$
\boldsymbol{s} : \mathbf{1} = 0 \qquad \text{and} \qquad \boldsymbol{s} : \boldsymbol{M}_F = 0.
\tag{3}
$$

Then, from (2) and (3) we deduce that

$$p = \frac{1}{2}\left(\text{tr}[\boldsymbol{\sigma}] - [\boldsymbol{\sigma} : \boldsymbol{M}_F]\right), \qquad T = \frac{1}{2}\left(3\left[\boldsymbol{\sigma} : \boldsymbol{M}_F\right] - \text{tr}[\boldsymbol{\sigma}]\right) \qquad (4)$$

and it follows by eliminating p and T from (2) that the second order tensor $\boldsymbol{s}$ can be written as $\boldsymbol{s} = \mathbb{P} : \boldsymbol{\sigma}$, where $\mathbb{P}$ is the fourth-order projection tensor given by

$$\mathbb{P} = \boldsymbol{I} - \frac{1}{2}\,\boldsymbol{1} \otimes \boldsymbol{1} - \frac{3}{2}\,\boldsymbol{M}_F \otimes \boldsymbol{M}_F + \frac{1}{2}\left(\boldsymbol{M}_F \otimes \boldsymbol{1} + \boldsymbol{1} \otimes \boldsymbol{M}_F\right) \qquad (5)$$

and where $\boldsymbol{I}$ is the fourth-order symmetric unit tensor with components $I_{ijkl} = (\delta_{ik}\delta_{jl} + \delta_{il}\delta_{jk})/2$. In the terminology employed by Spencer (1984), $\boldsymbol{s}$ is called the extra-stress tensor. Notice that if the condition $(3)_2$ were not imposed, $\boldsymbol{s}$ would become the well known deviatoric stress tensor and p the hydrostatic pressure.

Likewise, in this work, the same decomposition as for the stress tensor in (2) is this time applied for the strain tensor. We write then

$$\boldsymbol{\varepsilon} = \boldsymbol{e} + \vartheta\,\boldsymbol{1} + \xi\,\boldsymbol{M}_F \qquad (6)$$

where, by analogy, we define $\boldsymbol{e}$ as the extra-strain tensor given by $\boldsymbol{e} = \mathbb{P} : \boldsymbol{\varepsilon}$, and where the scalar strain quantities ϑ and ξ are similarly obtained by imposing the conditions $\boldsymbol{e} : \boldsymbol{1} = 0$ and $\boldsymbol{e} : \boldsymbol{M}_F = 0$.

With these decompositions at hand, replacing the identities (2) and (6) in the constitutive equation (1), one can extract the following remarkable extra-stress-strain relation

$$\boldsymbol{s} = 2\mu_T\,\boldsymbol{e} + 2(\mu_L - \mu_T)\left\{\boldsymbol{M}_F\,\boldsymbol{e} + \boldsymbol{e}\,\boldsymbol{M}_F\right\}. \qquad (7)$$

Notice that this latter depends *only* on the shear moduli μ_L and μ_T. This important fact will be exploited later for the viscoelastic shear modelling. Also, for later use, this relation is equivalently written as

$$\boldsymbol{s} = \underbrace{\left[2\mu_T\,\boldsymbol{I}\,+\,2(\mu_L-\mu_T)\,\boldsymbol{I}_F\right]}_{=\,\boldsymbol{\mathsf{C}}_s} : \boldsymbol{e} \tag{8}$$

where $\boldsymbol{\mathsf{C}}_s$ is the fourth-order transversely isotropic elastic shear tensor. The fibre-direction-dependent fourth-order tensor $\boldsymbol{I}_F$ is such that $\boldsymbol{I}_F : \boldsymbol{A} = \boldsymbol{M}_F\,\boldsymbol{A} + \boldsymbol{A}\,\boldsymbol{M}_F$ for every symmetric second order tensor $\boldsymbol{A}$. Its components are given by

$$(\boldsymbol{I}_F)_{ijkl} = \frac{1}{2}\left(V_{F_i}V_{F_k}\delta_{jl} + V_{F_i}V_{F_l}\delta_{jk} + V_{F_j}V_{F_l}\delta_{ik} + V_{F_k}V_{F_j}\delta_{il}\right). \tag{9}$$

Also from the constitutive equation (1), one obtains the complementary stress-strain relations for the scalar quantities $(p, T) - (\vartheta, \xi)$, written for convenience in matrix form as

$$\left\{\begin{array}{c} p \\ T \end{array}\right\} = \left[\begin{array}{cc} 3\lambda + 2\mu_T + \alpha & \lambda + \alpha \\ \beta + 4(\mu_L - \mu_T) + 3\alpha & \beta + 4\mu_L - \mu_T + \alpha \end{array}\right]\left\{\begin{array}{c} \vartheta \\ \xi \end{array}\right\}. \tag{10}$$

3. Time-dependent behaviour by matrix shear creep

Now we consider that the material has a viscoelastic response. For fibre-reinforced materials, the role of the matrix is to deform and support stresses primarily in shear. We then expect the matrix to be viscoelastic in *shear*. Moreover, it is also reasonable to expect that the fibres remain time-independent and linearly elastic. The key idea in this work is that these conditions can be incorporated by assuming the constitutive relation be viscoelastic *only* through its extra-stress-strain part as given by (7). This choice

7

is motivated by the fact that the extra-stress tensor $\boldsymbol{s}$ and the extra-strain tensor $\boldsymbol{e}$ are related only by the material parameters μ_L and μ_T which capture the shear behaviour of the composite material.

In the following we characterize such a behaviour by means of an internal variable model. A description solely via external variables is also possible. Hence we write

$$\boldsymbol{s} = \mathbf{C}_s : (\boldsymbol{e} - \boldsymbol{e}^{\mathrm{v}}) \tag{11}$$

where the newly introduced strain-like internal variable $\boldsymbol{e}^{\mathrm{v}}$ is the viscous part of the strain tensor. This latter is not accessible to direct observation and can in turn be the sum of as many as necessary internal contributions $\boldsymbol{e}_i^{\mathrm{v}}$, *i.e.*

$$\boldsymbol{e}^{\mathrm{v}} = \sum_{i=1}^{m} \boldsymbol{e}_i^{\mathrm{v}} \tag{12}$$

where the $i = 1, \ldots m$ hidden tensor variables $\boldsymbol{e}_i^{\mathrm{v}}$ characterize viscoelastic processes with corresponding relaxation times $\tau_i \in (0, \infty)$, $i = 1, \ldots m$. The complementary part of the total stress-strain relation is kept (time-independent) *fully* elastic. That is, the scalar stress-strain relations (10) remain unchanged.

Now, in order to describe the way the viscoelastic process evolves, it is necessary to specify complementary equations that govern the evolution of the internal variables $\boldsymbol{e}_i^{\mathrm{v}}$, $i = 1, \ldots m$. In this work, these evolutions are motivated by the following well known generalized Kelvin-Voigt rheological model. Of course, other choices are also possible.

3.1. One-dimensional rheological model

The rheological model of Figure 1 displays both relaxation and creep behaviour. It consists of a free spring on one end and an arbitrary number m

8

of Kelvin elements arranged in series. The stiffnesses of the free spring and the i-spring elements are $E > 0$ and $E_i > 0$, $i = 1, \ldots m$, respectively. And the viscosity of the i-dashpot elements are specified by the material constants $\eta_i > 0$, $i = 1, \ldots m$.

Figure 1: One-dimensional rheological model.

Now the governing equations for the generalized Kelvin-Voigt model depicted in Figure 1 are derived by elementary considerations. Let σ be the stress applied to the whole model and ε be the external total strain. The stress on each i-spring is $E_i \, \varepsilon_i^{\mathrm{v}}$, and the stress on each corresponding i-dashpot is given by the linear relation $\eta_i \, \dot{\varepsilon}_i^{\mathrm{v}}$, where the upper dot $(\dot{\;})$ is the time derivative. Hence, on the one hand, the resultant stress in each i-Kelvin element (an i-spring in parallel with an i-dashpot) is the sum $E_i \, \varepsilon_i^{\mathrm{v}} + \eta_i \, \dot{\varepsilon}_i^{\mathrm{v}}$. And on the other hand, since the strain on the free spring is $\varepsilon - \varepsilon^{\mathrm{v}}$, where $\varepsilon^{\mathrm{v}} = \sum_{i=1,m} \varepsilon_i^{\mathrm{v}}$, the stress on this spring is given by $E \left(\varepsilon - \varepsilon^{\mathrm{v}} \right)$.

The free spring and all the m Kelvin elements being connected in series, then by equilibrium the stress is found to be given by any of the following m equations

$$\sigma = E \left(\varepsilon - \varepsilon^{\mathrm{v}} \right) = E_i \, \varepsilon_i^{\mathrm{v}} + \eta_i \, \dot{\varepsilon}_i^{\mathrm{v}}, \qquad i = 1, \ldots m, \tag{13}$$

where no sum on the indices i is assumed. Now denoting by $\tau_i = \eta_i / E_i > 0$, $i = 1, \ldots m$ the relaxation times, and by $\omega_i > 0$ $i = 1, \ldots m$ the stiffness factors such that $E_i = E / \omega_i$, $(13)_2$ implies the important m evolution equations

$$\dot{\varepsilon}_i^{\mathrm{v}} + \frac{1 + \omega_i}{\tau_i} \varepsilon_i^{\mathrm{v}} + \frac{\omega_i}{\tau_i} \sum_{j=1, j \neq i}^{m} \varepsilon_j^{\mathrm{v}} = \frac{\omega_i}{\tau_i} \varepsilon, \qquad i = 1, \ldots m \tag{14}$$

for the internal variables $\varepsilon_i^{\mathrm{v}}$, $i = 1, \ldots m$.

3.2. Three-dimensional evolution equations

We motivate the evolution equations for the three-dimensional deformation by reference to the relationship (14). An obvious choice of appropriate evolution equations for the internal variables e_i^{v} is given by

$$\dot{e}_i^{\mathrm{v}} + \frac{1+\omega_i}{\tau_i}\, e_i^{\mathrm{v}} + \frac{\omega_i}{\tau_i} \sum_{j=1,j\neq i}^{m} e_j^{\mathrm{v}} = \frac{\omega_i}{\tau_i}\, e, \qquad i = 1, \ldots m \qquad (15)$$

where τ_i, $i = 1, \ldots m$ are the relaxation times and the dimensionless factors ω_i, $i = 1, \ldots m$ are material parameters. Notice that, except for the case of a simple Kelvin-Voigt model with $m = 1$, the m evolution equations (15) are all coupled since each single internal variable e_i^{v} appears in all the m equations. Notice also that if the m factors ω_i are set to zero, then no viscous evolution takes place and the material response remains linearly elastic.

Last but not least, it emerges from the structure of the m equations (15) that, by construction, the internal strain-like tensors e_i^{v}, $i = 1, \ldots m$ satisfy the conditions $e_i^{\mathrm{v}} : \mathbf{1} = 0$ and $e_i^{\mathrm{v}} : \boldsymbol{M}_F = 0$ as does the extra-strain tensor $\boldsymbol{e}$ which appears on the right hand side of (15).

In summary: the phenomenological matrix creep fibre-reinforced model is described by the constitutive equations (2), (10)-(12) and the m evolution equations (15).

4. Time integration and numerical implementation

Within the finite element method, the (local) evolution equations (15) must be solved locally at the integration points level through a strain-driven type of numerical procedure. Consider a typical time interval $[t_n, t_{n+1}]$, an arbitrary material point $\boldsymbol{x}$ and assume that the variables $e_{i\,n}^{\mathrm{v}}$, $i = 1, \ldots m$

are known prescribed initial data on $\boldsymbol{x}$ at time t_n. The objective is then to approximate the m equations (15) to advance the solution to time t_{n+1} and update the variables to $\boldsymbol{e}^{\mathrm{v}}_{i\,n+1}$ for a fixed increment of deformation.

Among the many possibilities, we propose in this paper two algorithms: a fully implicit scheme, and an explicit scheme combined with the exponential map. In all cases, the discrete versions of (15) are always *linear*.

4.1. Implicit time integration scheme

The implicit backward-Euler scheme applied to (15) gives a linear system of m *coupled* equations

$$
\begin{aligned}
\omega_i \, \Delta t \, \boldsymbol{e}^{\mathrm{v}}_{1\,n+1} \quad + \ldots + \quad & (\tau_i + (1+\omega_i)\Delta t)\, \boldsymbol{e}^{\mathrm{v}}_{i\,n+1} \\
+ \ldots + \quad & \omega_i \, \Delta t \, \boldsymbol{e}^{\mathrm{v}}_{m\,n+1} \; = \; \omega_i \, \Delta t \, \boldsymbol{e}_{n+1} \; + \; \tau_i \, \boldsymbol{e}^{\mathrm{v}}_{i\,n}
\end{aligned}
\tag{16}
$$

$i = 1, \ldots m$, where $\boldsymbol{e}_{n+1}$ is the *known* (total) extra-strain tensor at time t_{n+1}, and where $\Delta t = t_{n+1} - t_n$ stands for the time increment. For computational purposes, the m equations (16) can be equivalently written in Voigt engineering notation as

$$
\tilde{\boldsymbol{H}}
\left\{
\begin{array}{c}
\tilde{\boldsymbol{e}}^{\mathrm{v}}_{1\,n+1} \\
\vdots \\
\tilde{\boldsymbol{e}}^{\mathrm{v}}_{i\,n+1} \\
\vdots \\
\tilde{\boldsymbol{e}}^{\mathrm{v}}_{m\,n+1}
\end{array}
\right\}
=
\left\{
\begin{array}{c}
\omega_1 \, \Delta t \, \tilde{\boldsymbol{e}}_{n+1} + \tau_1 \, \tilde{\boldsymbol{e}}^{\mathrm{v}}_{1\,n} \\
\vdots \\
\omega_i \, \Delta t \, \tilde{\boldsymbol{e}}_{n+1} + \tau_i \, \tilde{\boldsymbol{e}}^{\mathrm{v}}_{i\,n} \\
\vdots \\
\omega_m \, \Delta t \, \tilde{\boldsymbol{e}}_{n+1} + \tau_m \, \tilde{\boldsymbol{e}}^{\mathrm{v}}_{m\,n}
\end{array}
\right\}
\tag{17}
$$

11

with $\tilde{\boldsymbol{H}}$ being the matrix of the system given by

$$
\tilde{\boldsymbol{H}} =
\begin{bmatrix}
(\tau_1 + (1+\omega_1)\Delta t)\,\tilde{\boldsymbol{I}} & \cdots & \omega_1 \Delta t\,\tilde{\boldsymbol{I}} & \cdots & \omega_1 \Delta t\,\tilde{\boldsymbol{I}} \\
\vdots & & \vdots & & \vdots \\
\omega_i \Delta t\,\tilde{\boldsymbol{I}} & \cdots & (\tau_i + (1+\omega_i)\Delta t)\,\tilde{\boldsymbol{I}} & \cdots & \omega_i \Delta t\,\tilde{\boldsymbol{I}} \\
\vdots & & \vdots & & \vdots \\
\omega_m \Delta t\,\tilde{\boldsymbol{I}} & \cdots & \omega_m \Delta t\,\tilde{\boldsymbol{I}} & \cdots & (\tau_m + (1+\omega_m)\Delta t)\,\tilde{\boldsymbol{I}}
\end{bmatrix}
\tag{18}
$$

where, and in all what follows, the tilde notation $(\tilde{.})$ refers to matrix and vector representations of fourth- and second-order tensors quantities in Voigt notation, respectively.

Useful when the present linear viscoelastic model is coupled to material nonlinearities such as plasticity and/or damage needing then iterative resolution strategies, is to express the extra-stress-strain constitutive relation (11) as a rate of change of $\boldsymbol{s}$ in terms of the *total* strain rate $\dot{\boldsymbol{\varepsilon}}$ via the algorithmic viscoelastic tensor. This is accomplished in two steps: in the first step, from the discrete form (17), we deduce the algorithmic change of the internal variables $\boldsymbol{e}_i^{\mathrm{v}}$, $i = 1, \ldots m$, in terms of the rate of change of the total extra-strain $\boldsymbol{e}$. In matrix form one obtains

$$
\left\{
\begin{array}{c}
\dot{\boldsymbol{e}}_1^{\mathrm{v}} \\
\vdots \\
\dot{\boldsymbol{e}}_m^{\mathrm{v}}
\end{array}
\right\}
= \tilde{\boldsymbol{H}}^{-1}
\begin{bmatrix}
\omega_1 \Delta t\,\tilde{\boldsymbol{I}} \\
\vdots \\
\omega_m \Delta t\,\tilde{\boldsymbol{I}}
\end{bmatrix}
\dot{\boldsymbol{e}}
\tag{19}
$$

and in the second step, replacing this expression in the rate form of (11): $\dot{\boldsymbol{s}} = \mathbf{C}_s : (\dot{\boldsymbol{e}} - \dot{\boldsymbol{e}}^{\mathrm{v}})$ where $\mathbf{C}_s$ has been defined in (8), together with the use of

12

the projection tensor $\mathbb{P}$ defined in (5), gives in matrix form

$$\tilde{\mathbf{C}}_s^{\text{algo}} = \left(\tilde{\mathbf{C}}_s - \underbrace{\left[\tilde{\mathbf{C}}_s \cdots \tilde{\mathbf{C}}_s \right]}_{m \ times} \tilde{\boldsymbol{H}}^{-1} \begin{bmatrix} \omega_1 \Delta t \, \tilde{\boldsymbol{I}} \\ \vdots \\ \omega_m \Delta t \, \tilde{\boldsymbol{I}} \end{bmatrix} \right) \tilde{\mathbb{P}} \qquad (20)$$

such that $\dot{\tilde{\boldsymbol{s}}} = \tilde{\mathbf{C}}_s^{\text{algo}} \dot{\tilde{\boldsymbol{\varepsilon}}}$.

Remark 1. In three-dimensional computations, the $(6\,m \times 6\,m)$ matrix $\tilde{\boldsymbol{H}}$ defined by equation (18) is constant $((3\,m \times 3\,m)$ in two dimensions). It is the same for each integration point with the same material properties and during the whole computational process. It needs then to be computed, inverted and stored only once whenever the time increment Δt is kept constant during the incremental process. $\qquad \square$

4.2. An explicit time integration scheme

For each evolution equation i in (15), setting the internal variables $\boldsymbol{e}_j^{\text{v}}$, $j = 1, \ldots m, j \neq i$ to their values at time t_n, and use of the exponential map on each of the resulting m *decoupled* equations give the following simple updates

$$\boldsymbol{e}_{i\,n+1}^{\text{v}} = \frac{\omega_i}{1 + \omega_i} \left\{ \boldsymbol{e}_{n+1} - \sum_{j=1, j \neq i}^{m} \boldsymbol{e}_{j\,n}^{\text{v}} \right\} (1 - \exp(-\alpha_i \, \Delta t)) + \boldsymbol{e}_{i\,n}^{\text{v}} \exp(-\alpha_i \, \Delta t)$$

(21)

$i = 1, \ldots m$, where we have introduced the notation $\alpha_i = (1 + \omega_i)/\tau_i$. In this case, the algorithmic change of the internal variables in terms of the rate of change of the total extra-strain is given by

$$\dot{\boldsymbol{e}}_i^{\text{v}} = \underbrace{\frac{\omega_i}{1 + \omega_i} (1 - \exp(-\alpha_i \, \Delta t))}_{= \, \beta_i} \dot{\boldsymbol{e}}, \qquad i = 1, \ldots m \qquad (22)$$

13

The algorithmic viscoelastic tensor is then such that

$$
\begin{aligned}
\dot{\boldsymbol{s}} &= \zeta\, \boldsymbol{\mathsf{C}}_s : \dot{\boldsymbol{e}} \\
&\equiv \underbrace{\zeta\, [2\mu_T\, \mathbb{P} \,+\, 2(\mu_L - \mu_T)\, \boldsymbol{I}_F \,+\, 4(\mu_L - \mu_T)\, \boldsymbol{M}_F \otimes \boldsymbol{M}_F]}_{=\,\boldsymbol{\mathsf{C}}_s^{\text{algo}}} : \dot{\boldsymbol{\varepsilon}} \qquad (23)
\end{aligned}
$$

with the notation $\zeta = \left(1 - \sum_{i=1,m} \beta_i\right)$, and where β_i, $i = 1, \ldots m$ are defined in (22). The fourth-order tensors $\mathbb{P}$ and $\boldsymbol{I}_F$ have been defined in (5) and (9), respectively.

Remark 2. As for all explicit time discretizations, care must be taken during the computations. That is, the values of the computational time increments Δt must be at least lesser than the smallest value among all the relaxation times τ_i, $i = 1, \ldots m$. $\qquad\square$

5. Numerical examples

The elastic constants of transversely isotropic materials are usually given by parameters which have more physical interpretations. If, for example, the fibres' direction coincides with the global $\vec{e}_1$-axis, the compliance elastic tensor is given in Voigt notation as

$$
\begin{bmatrix}
1/E_1 & -\nu_{12}/E_1 & -\nu_{12}/E_1 & & & \\
-\nu_{12}/E_1 & 1/E_2 & -\nu/E_2 & & & \\
-\nu_{12}/E_1 & -\nu/E_2 & 1/E_2 & & & \\
& & & 1/G_{12} & & \\
& & & & 1/G_{12} & \\
& & & & & (1+\nu)/E_2
\end{bmatrix}
\qquad (24)
$$

where E_1 and E_2 are the Young's moduli in the directions parallel and normal to the fibres, respectively, G_{12} and ν_{12} are the shear modulus and Poisson's

14

ratio on planes parallel to the fibres, and ν is the Poisson's ratio on the plane normal to the fibres (the plane spanned by $(\vec{e}_2, \vec{e}_3)$ in this example). And for this fibres' direction, the constitutive equation (1) gives the following corresponding stiffness elastic tensor

$$
\begin{bmatrix}
\lambda + 2\alpha + 4\mu_L - 2\mu_T + \beta & \lambda + \alpha & \lambda + \alpha & & & \\
\lambda + \alpha & \lambda + 2\mu_T & \lambda & & & \\
\lambda + \alpha & \lambda & \lambda + 2\mu_T & & & \\
& & & 2\mu_L & & \\
& & & & 2\mu_L & \\
& & & & & 2\mu_T
\end{bmatrix}
\tag{25}
$$

Inspection of these two matrices immediately gives

$$
\mu_L = \frac{G_{12}}{2} \qquad \text{and} \qquad \mu_T = \frac{E_2}{2(1+\nu)}
\tag{26}
$$

and the remaining constants are easily obtained by inverting the first 3×3 bloc-matrix of (24), equalizing the result with the first 3×3 bloc-matrix of (25), and then solving for λ, α and β. Notice again that within the present coordinate-free formulation, the fibres' direction is not necessary the same at each point. The composite is in fact *locally* transversely isotropic with respect to the local fibres' direction which is a known function of position, *i.e.* $\vec{V}_F = \vec{V}_F(\boldsymbol{x})$.

Remark 3. A particular transversely isotropic behaviour can be obtained with elastic constants such that $\alpha = 0$ and $\mu_L = \mu_T \equiv \mu$. This is widely employed in the finite strain range modelling of fibre reinforced composites. In particular, it permits an easy account of the reinforcements when more than one family of fibres have to be accounted for (more than one fibres' direction)

15

and falls then within the scope of strongly anisotropic solids. See for example (Nedjar, 2007) for the case of finite strain anisotropic viscoelasticity.   □

5.1. Matrix-creep for slight off-axis loadings

In this first example, the sensitivity of the model to predict the influence of the fibre direction on the overall viscoelastic behaviour is discussed through a creep loading example. As the unidirectional composites are mainly designed to carry loads in the fibre direction, we analyze situations where slight off-axis loadings can occur as a result of unperfect alignement between fibres' and loading directions.

We consider the $(100 \times 50)\,mm^2$ rectangular specimen of Figure 2. The boundary conditions are such that the right edge is loaded by imposing a uniform horizontal traction along the $\vec{e}_1$-axis. Within the finite element method, the middle node of the left edge is fixed in the vertical direction to avoid any rigid body motion. The family of fibres is characterized by the angle θ with respect to the $\vec{e}_1$-direction.

Figure 2: Slight off-axis loading influence. Geometry and boundary conditions.

For the composite material, we use the following elastic characteristics: $E_L = 138\,GPa$, $E_T = 9.8\,GPa$, $G_{LT} = 5.9\,GPa$, $\nu_{LT} = 0.305$ and $\nu_T = 0.019$, where the subscript L refers to the fibres' direction and T refers to the transverse plane normal to it. Those values correspond to usual unidirectional carbon-epoxy fibre-reinforced composites, see for example (Kawai et al.,

2001). Within the present formulation, they lead to the following Lamé-like elastic constants (in GPa):

$$\lambda = 0.254 \qquad \mu_T = 4.808 \qquad \mu_L = 2.95 \qquad \beta = 131.778 \qquad \alpha = 2.834$$

For the *shear* viscous part of the behaviour, we choose three viscoelastic mechanisms with the following couples of parameters

$$(\tau_1 = 10, \omega_1 = 0.5) \qquad (\tau_2 = 1000, \omega_2 = 2) \qquad (\tau_3 = 10000, \omega_3 = 4)$$

where the relaxation times τ_i, $i = 1, 2, 3$ are given in unit of time.

Figure 3 shows the results of a series of creep tension tests at $200\,MPa$ for different off-axis angles, here for $\theta = 3°, 5°$ and $10°$, and superposed with the case of co-axiality, *i.e.* with $\theta = 0°$. They represent the evolution of the global ε_{11}-strain component with respect to time. These results clearly show the strong influence of the fibres' direction on the global behaviour of the streep even for small deviations of the loading away from the direction of the fibres. In fact, compared to the co-axial case, the relative strain is about $100\,\%$ for $\theta = 5°$ and $400\,\%$ for $\theta = 10°$ at the end of the creep computations.

Figure 3: Composite creep results for slight off-axis tensions. A load of $200\,MPa$ is applied in the $\vec{e}_1$-direction.

Remark 4. In this two-dimensional example, the response of the material is still time-dependent for co-axial loadings, but the weight of the viscoelastic part of the response over the total response is very small as the composite material is very stiff in the direction of the fibres. □

5.2. Matrix-creep with the presence of an imperfection

In this second example, we study the creep of a unidirectional composite globally loaded in the direction of the fibres when an imperfection is locally present in the specimen. Obviously, such an imperfection locally deviates the co-axiality of the fibres with respect to the loading direction. For the sake of simplicity, we assume that the local volume fraction of the fibres remains unchanged around the imperfection so that the same local transversely isotropic material properties can be used.

We consider the $(50 \times 100) \, mm^2$ rectangular specimen of Figure 4 uniformly loaded in traction along the $\vec{e}_2$-direction, and where the imperfection is repesented by a circular hole of radius R at the center of the sample. The family of fibres is deviated from the vertical direction along the lines given by (notice the analogy with stream lines in fluid mechanics)

$$x_1 - \frac{R^2 \, x_1}{x_1^2 + x_2^2} = Cte \tag{27}$$

where x_1 and x_2 are the coordinates with respect to the global basis $(\vec{e}_1, \vec{e}_2)$ centered for convenience at the center of the circular hole. The fibres' direction field is then given by

$$\vec{V}_F = \left\{ \begin{array}{c} \zeta_1/(\zeta_1^2 + \zeta_2^2)^{1/2} \\ \zeta_2/(\zeta_1^2 + \zeta_2^2)^{1/2} \end{array} \right\} \tag{28}$$

where

$$\zeta_1 = -2R^2 \frac{x_1 x_2}{(x_1^2 + x_2^2)^2} \qquad \zeta_2 = 1 + R^2 \frac{x_1^2 - x_2^2}{(x_1^2 + x_2^2)^2} \tag{29}$$

Notice that away from the circle, the fibres' direction tends to $\vec{V}_F = \langle 0, 1 \rangle^T$, i.e. co-axiality with the loading direction.

Figure 4: Composite creep with the presence of a circular imperfection. Geometry and boundary conditions.

Remark 5. For a material point $\boldsymbol{x}$, with components (x_1, x_2), that belongs to the interior of the circle, *i.e.* when $r \equiv (x_1^2 + x_2^2)^{1/2} \leq R$, its fibre's direction is given by the tangent to the circle of radius R at its radially projected point on that circle. That is, the unit vector $\vec{V}_F$ in (28) is computed with

$$\zeta_1 = -\frac{R}{r} x_2 \qquad \zeta_2 = \frac{R}{r} x_1 \tag{30}$$

Notice that within the finite element framework, the fibres' directions are computed at the integration points level. $\square$

Figure 5 shows the results of a series of creep tension tests at $300\,MPa$ for different values of the radius R. Notice that the case $R = 0$ corresponds to the absence of any imperfection. For the composite, the material characteristics are those used in the precedent example (in Section 5.1).

Figure 5: Composite creep results for different values of the circular imperfection's radius R. A load of $300\,MPa$ in tension is applied in the $\vec{e}_2$-direction.

From these curves, one can notice the influence of the dimension of the imperfection on the overall creep response of the specimen. By deduction, one can extrapolate that with more imperfections in the specimen, the creep response would be more noticeable.

6. Conclusion and perspectives

In this paper, a viscoelastic formulation for fibre-reinforced composite materials with one family of fibres has been presented. It focuses on the homogeneous macroscopic material level in order to provide a tool for structural finite element simulations.

The anisotropic response has been captured with the locally transversely isotropic formulation as proposed by Spencer (1984) where the constitutive relation can be decomposed into a volumetric, a fibre-directional, and an extra-stress-strain parts. As it is observed that creep mainly occurs in the matrix phase due to shear, the rate-dependent part of the behaviour is then captured only through the extra-stress-strain part. It has been shown through representative finite element simulations that the present model is able to capture high creep influence on the response of composite structures when slight off-axis loadings are applied. And when imperfections are present in the structures (these are mainly due to the fabrication process), it has also been shown that the model can take into account their influence on the global structural response.

In general, the composite materials exhibit marked plastic behaviour which can be combined to damage as fibres can break when a certain threshold of loading is reached. Among the abundant literature, see for example (Beyerlein et al., 1998; Kawai et al., 2001; Ohno et al., 2002; Sun and Chen, 1989) among many others. The model developed in this paper is linearly elastic and linearly viscoelastic which limits its field of application. Its extension to take into account damage and/or (visco)plasticity is the object of a future work.

References

Beyerlein, I., Phoenix, S., Raj, R., 1998. Time evolution of stress redistribution around multiple fiber breaks in a composite with viscous and viscoelastic matrices. International Journal of Solids and Structures **35**(24), 3177–3211.

Bonet, J., Burton, A., 1998. A simple orthotropic, transversely isotropic hyperelastic constitutive equation for large strain computations. Computer Methods in Applied Mechanics and Engineering **162**, 151–164.

Holzapfel, G., 2000. Nonlinear solid mechanics. A continuum appraoch for engineering. John Wiley and Sons, Ltd, Chichester, West Sussex, UK.

Kaliske, M., 2000. A formulation of elasticity and viscoelasticity for fibre reinforced material at small and finite strains. Computer Methods in Applied Mechanics and Engineering **185**, 225–243.

Kawai, M., Masuko, Y., Kawase, Y., Negishi, R., 2001. Micromechanical analysis of the off-axis rate-dependent inelastic behavior of unidirectional AS4/PEEK at hight temperature. International Journal of Mechanical Science **43**, 2069–2090.

Klinkel, S., Sansour, C., Wagner, W., 2005. An anisotropic fibre-matrix material model at finite elastic-plastic strains. Computational Mechanics **35**, 409–417.

Nedjar, B., 2007. An anisotropic viscoelastic fibre-matrix model at finite strains: Continuum formulation and computational aspects. Computer Methods in Applied Mechanics and Engineering **196**(9-12), 1745–1756.

Ohno, N., Ando, T., Miyake, T., Biwa, S., 2002. A variational method for unidirectional fiber-reinforced composites with matrix creep. International Journal of Solids and Structures **39**, 159–174.

Reese, S., 2003. Meso-macro modelling of fibre-reinforced rubber-like composites exhibiting large elastoplastic deformation. International Journal of Solids and Structures **40**, 951–980.

Reese, S., Raible, T., Wriggers, P., 2001. Finite element modelling of orthotropic material behaviour in pneumatic membranes. International Journal of Solids and Structures **38**, 9525–9544.

Sansour, C., Karsaj, I., Soric, J., 2006. A formulation of anisotropic continuum elastoplasticity at finite strains. Part I: Modelling. International Journal of Plasticity **22**, 2346–2365.

Spencer, A., 1984. Constitutive theory for strongly anisotropic solids, in: Spencer, A. (Ed.), Continuum theory of the mechanics of fibre-reinforced composites, CISM cources and lectures No. 282, Springer, Wien.

Sun, C., Chen, J., 1989. A simple flow rule for characterizing nonlinear behavior effect of fiber composites. Journal of Composite Materials **23**, 1009–1020.

Weiss, J., Maker, B., Govindjee, S., 1996. Finite element implementation of incompressible, transversely isotropic hyperelasticity. Computer Methods in Applied Mechanics and Engineering **135**, 107–128.

Figure captions

- Fig. 1: One-dimensional rheological model.

- Fig. 2: Slight off-axis loading influence. Geometry and boundary conditions.

- Fig. 3: Composite creep results for slight off-axis tensions. A load of $200\,MPa$ is applied in the $\vec{e}_1$-direction.

- Fig. 4: Composite creep with the presence of a circular imperfection. Geometry and boundary conditions.

- Fig. 5: Composite creep results for different values of the circular imperfection's radius R. A load of $300\,MPa$ in tension is applied in the $\vec{e}_2$-direction.
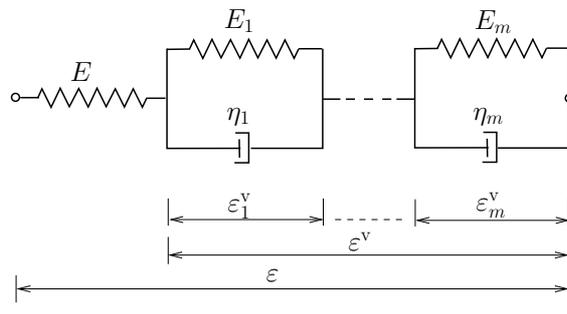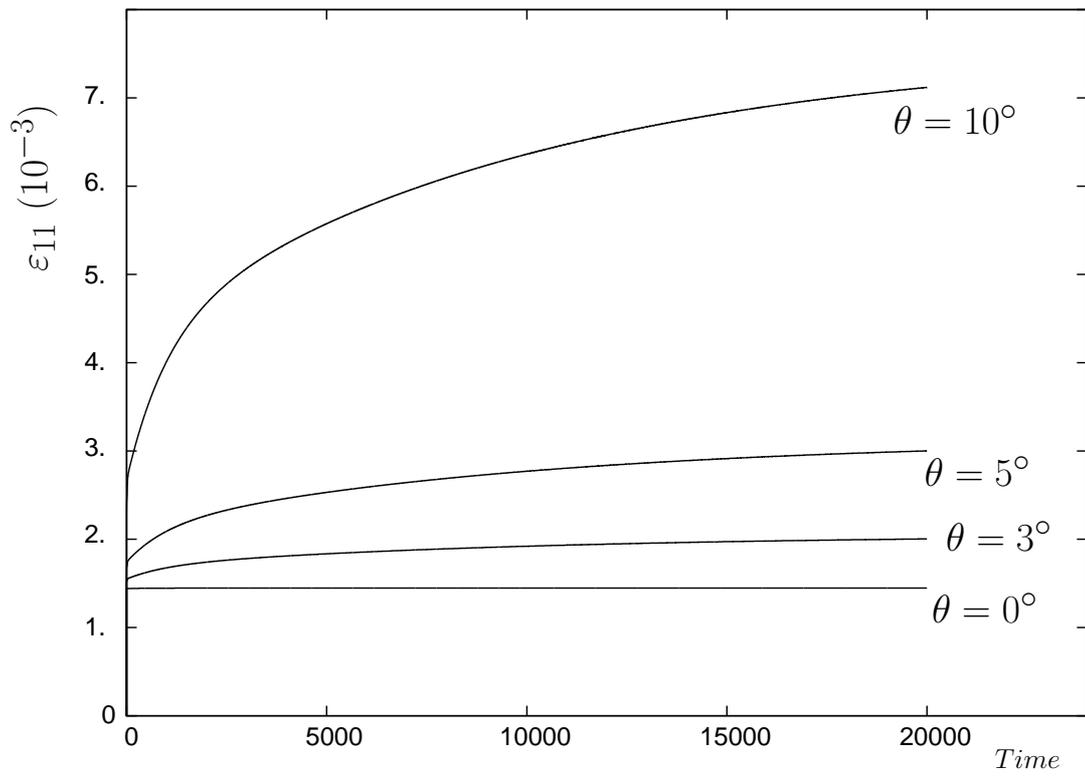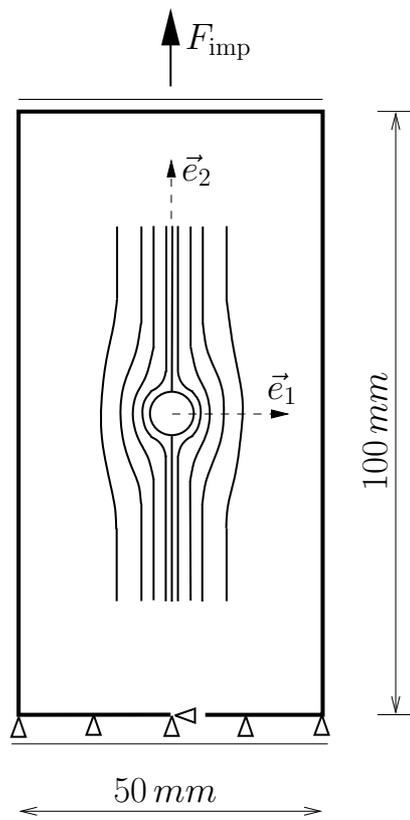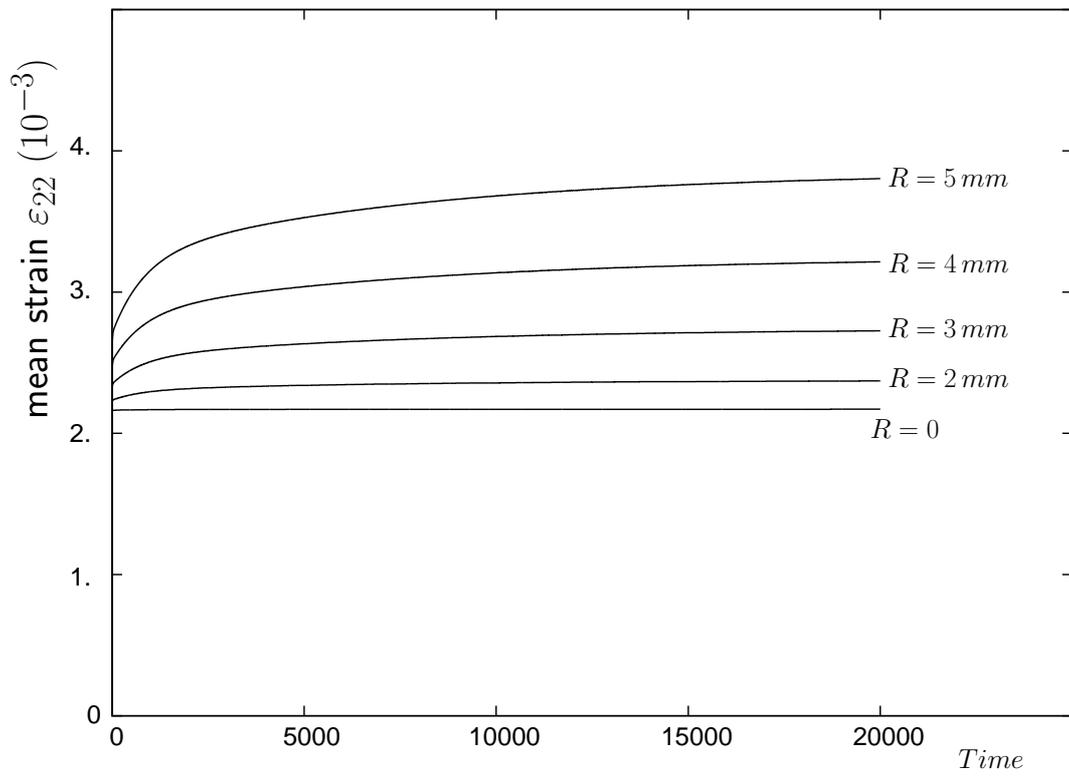
Figure 1:
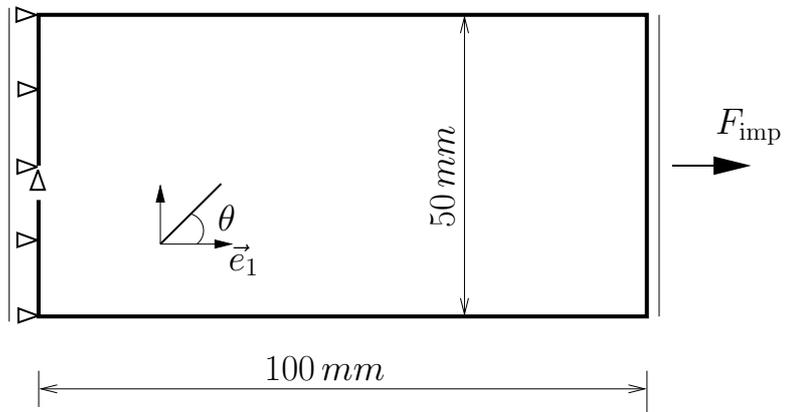
Figure 2:

Figure 3:

Figure 4:

Figure 5:

28